Development of an In-house Computer Code for the Simulation of Detonation Shock Dynamics in Underwater Explosion Scenario

P. Chellapandi[#] and C. Lakshmana Rao

Indian Institute of Technology, Madras, Chennai - 600 036, India
[#]*E-mail: perumalchellapandi@gmail.com*

ABSTRACT

Detonation Shock Dynamics (DSD), involved in an underwater explosion scenario is numerically simulated by an in-house computer code, 'DSSDYN'. The simulation is based on Chapman-Jouguet (CJ) theory, formulated in Arbitrary Lagrangian Eulerian frame work. Specifically, the propagation of detonation front is simulated with 'Burn Fraction Model'. The classical burn fraction model is improved for achieving better computational efficiency. The simulation capability of DSS-DYN is demonstrated through a case study on explosion of PETN charge under the deep-water medium. Through this study, the salient features of DSD with better insight have been brought out. Besides, the physical parameters, such as work potential of PETN, are predicted efficiently. The apportionment of energy distributions indicates that about 70 % of chemical energy of explosive is transmitted to the surrounding water that is the major contribution of damage potential of the explosive. The predictions of peak velocity and peak pressure values by DSS-DYN and LS-DYNA show satisfactory comparison. DSS-DYN consumes lesser computational time (~1h), compared to LS-DYNA (~3h).

Keywords: Numerical simulation; Underwater explosion; Detonation shock dynamics; CJ theory; Burn fraction model; Energy distributions; Work potential of explosive

1. INTRODUCTION

Assessment of damage to the structures and systems subject to chemical explosions has several applications in civilian, nuclear and defence sectors. The numerical simulation of this problem involves a coupled treatment of (i) detonation process (ii) shock wave propagation and (iii) shock structure interactions. Detonation wave is basically a shock wave in a reactive medium behind which the chemical reaction takes place and the energy released in this reaction drives the shock wave forward, thereby creating oscillating pressure spikes of higher strength within the explosive boundary.

The associated and allied mechanical and chemical physics aspects are comprehensively covered under a topic called Detonation Shock Dynamics (DSD). The understanding of DSD is the essential step to predict the characteristics of detonation wave and its damage potential. Basics of detonation theory, experimental and numerical simulations are widely covered in several literatures, ref[1-6] are a few to name.

Several advances have been made on the experimental techniques to measure the conventional parameters relevant to underwater shock wave propagation phenomena.[6] However, inadequacy is still felt to measure certain key parameters for further understanding of DSD, specifically the rapid rate processes involving ultrahigh pressure peaks (typically 10-100 GPa) occurring in Nano to micro seconds. Alternatively, the numerical simulation is the most appropriate and efficient way to predict them realistically, by exploiting the current potential of numerical techniques and tools. The simulation should consider specifically large geometrical distortions and material damages in the internal and external structures. The commercial computer codes that are now available are AUTODYN,[7] LS-DYNA,[8] ABAQUS,[9] and DYTRAN.[10] These apart, a few 1D and 2D codes based on finite difference method employing weighted non-oscillatory scheme are available.[11] Specifically, AUTODYN and LS-DYNA are the most commonly used finite element codes for simulation of detonation with various explosives, shock wave propagation and ultimately structural damage deformation and damage computations.[12-16]

In the case of underwater explosion, the pressure waves originated from the detonation in the explosive cause significant damage to the structures housing the liquid as well as immersed in the liquid. The extent of the damage depends upon the strength of the pressure wave, which in turn depends upon the location of structures from the centre of detonation front, apart from its own characteristics and mass. Specifically, the nature and extent of damage to the structure could be quite different if they are placed close to liquid interface (near-field effects), compared to the damage to the similar structures if they are located far away from the interface (far-field effects). While the far-field effects on the structures have been studied elaborately both through experimental and numerical simulations,[12-14,17-18] near field effects in the case of underwater explosion are not addressed adequately. Among these, the references[15-16,18] are related to the open-air explosion. This is the motivation to undertake

the investigation on the near-field effects in the underwater explosion and this paper presents the outcome of the studies. The numerical simulation has been performed with an in-house computer code called 'DSS-DYN' developed by the authors. The prediction ability is demonstrated through a case study on explosion of a spherical shaped PETN (Penta Erythritol Tetra Nitrate), a representative high explosive, surrounded by infinite water medium.The paper has six sections: (1) introduction, (2) Highlights of underwater explosion scenario and DSD model conceptualized by Chapman-Jouguet (CJ) depicting the near-field and far-field effects, (3) highlights of the computer code DSS-DYN developed for hydrodynamic computations and numerical algorithm for burn fraction model(4) input details of benchmark problem chosen for the case study including equations of a state, (5) results and discussions and (6) conclusions.

The DSS-DYN has been developed to meet the objective of indigenization of high computational tools with freedom to apply for the strategic applications employing our own data bank. Nevertheless, attempt has been made to achieve higher computational efficiency.

2. UNDERWATER EXPLOSION SCENARIO
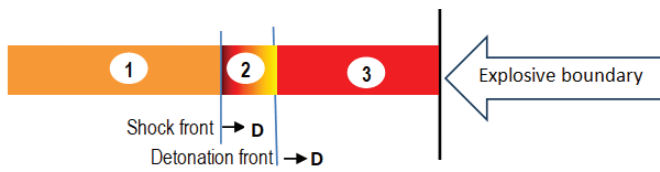
Sketch 1. Schematic sketch of underwater explosion scenario.

Referring the Sketch 1, an idealized model postulates three zones: (1) burnt product zone (2) a reactive zone and (3) un-burnt explosive, separated by detonation and shock fronts as in the adjoining shown. Thus, the detonation front converts the solid explosive into gaseous reaction products. A steady state equilibrium condition prevails till the detonation front reaches the explosive boundary. This means that the detonation and shock front velocities are same (D). The detonation velocity generally ranges from 6000-8000 m/s depending upon the explosive characteristics. In the burnt product zone, a non-stationary rarefaction takes place being controlled by the boundary conditions of the explosive charge. The composition of burnt products may change as a function of p, V, T, but no energy can be transferred to zones (1) & (2) and influence the characteristics of the detonation.The set of the conservation equations to be solved in building the model neglect the conductive and radiation effects and assume a laminar, non-viscous flow. As per a simplified detonation scenario conceptualized by Chapman-Jouguet (CJ), the release of chemical energy is complete and instantaneous. The time taken for the complete detonation within a typical explosive would be order of a few microseconds. The burnt products are assumed to behave as a homogeneous gas undergoing adiabatic thermodynamic process defined by Jones-Wilkins-Lee (JWL) equation of state,[19] commonly used for the numerical simulations for a range of explosives with the associated parameters quantified through curve fitting of experimental

data.[20] With the above postulations, simulation is simplified with the introduction of discontinuity of thermodynamic properties across the detonation front. Subsequently, the conventional hydrodynamic equations are derived from mass, momentum and energy balances and solved with an appropriate equation of state.

Upon completion of detonation, the pressure wave propagating in the liquid has oscillating pressure spikes emanating from the boundary due to the mechanical impact effects. The pressure spikes are restricted to the thin layers of explosive and liquid zones in the vicinity of the gaseous-liquid interface. An immediate consequence is the high velocity of material particles due to the large pressure gradient across the interface. The accumulated pressure and kinetic energies contribute to the work potential of the given explosion. In order to predict such in-depth aspects of DSD accurately, one should use fine computational mesh especially in the explosive and liquid zones around the interface. The shock/pressure waves propagating in the water away from the interface could causes damage to structures immersed in the surrounding liquid. A numerical simulation performed with TNT, PETN, C4 and SEP indicates that the transition between near-field and far-field effects, depends upon the charge radius, irrespective of the explosive type.[21] Further, it is concluded that the near-field effects exist up to distance of 2.5 times that of charge radius in water field.Beyond that, only far-field effects are seen. In the ref,[22] the far-field effects are investigated based on the thermo-chemical calculations carried out using EXPLO5 code for the selected explosive mixture. The effect of different aluminium weight percentage has been investigated based on the underwater experiments.

3. HIGHLIGHTS OF COMPUTER CODE: DSS-DYN

The basic version of DSS-DYN adopts homogenous model for the explosive ignoring the DSD effects.The detailed mathematical formulations, numerical integration procedures and validation are given in ref.[23] DSS-DYN has been extended to include the simulation of DSD for the various high-density explosives by adopting a 'Burn Fraction Model'

The model has been developed based on simplified concept postulated by CJ theory as illustrated in the schematic Sketch 1 shown under the Section 2. As per CJ theory, the detonation front moves with a constant velocity (D) and the front moves normal to the radial line originated from the point where the detonation got initiated. By this model, propagation of reactive zone is mapped, thereby to determine the burn fraction {F}. F is the ratio of burnt volume to the total volume of the element (V) In the finite element discretisation of the geometry, the detonation front should sweep element by element: typically, one 8-noded solid element (i^{th}) to the adjacent 8-noded solid element (j^{th}) lying in the outward radial line. For the purpose of numerical simplification, it is convenient to assume that the front sweeps one solid element during the travel between the centres of two adjacent elements (i^{th} to j^{th}). As per this, if t_i is the arrival time of the front for the ith element and t_j is the arrival time for the jth element, then the travel time for sweeping the volume of one complete solid element is (t_j-t_i).

The arrival time (t_i) is the time taken by the front starting from the detonation point, to reach the centroid of the ith element and similarly t_j is defined for j^{th} element. During the travel time between i^{th} to j^{th} element $(t_j - t_i)$, the projected area of ith element on the detonation front sweeps and burns the enclosed volume. These assumptions are in-line with the methodology adopted in ref[8,24] for computing the burn fraction. The projected area changes continuously during its travel from element to element. For overcoming this problem in a robust way, the following steps are implemented:

- The burn fraction (F) is computed based on the heat input to the volume.
- For the estimation of F for the ith element of volume (V_i), the radius of the equivalent sphere (r_i) is equal to $(3V_i / 4\pi)^{1/3}$ [Fig.1(a)].
- With the maximum projected area (A_i), equal to πr_i^2, the volume swept by the detonation front while moving radially with the velocity D at any time 't' is equal to volume of solid cylinder [section area $= A_i$ & height $= D(t - t_i)$ for '$t \le t_j$' : $V_{cylinder} = A_i D(t_j - t_i)$. [Fig.1(b)].
- Since, volume of sphere is $2/3^{rd}$ volume of enclosing cylinder, $V_{sphere} = 2/3 A_i D(t - t_i)$. V_{sphere} represents the burnt volume.
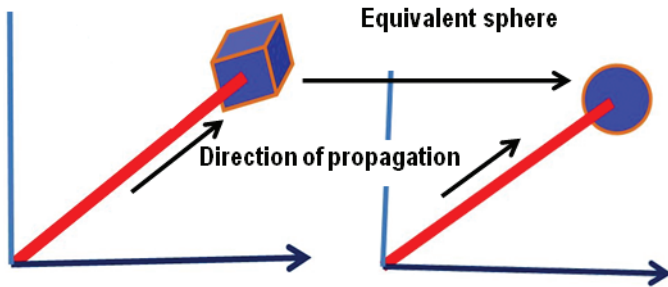
(a) Idealization of burning volume of arbitrary geometry into an equivalent sphere
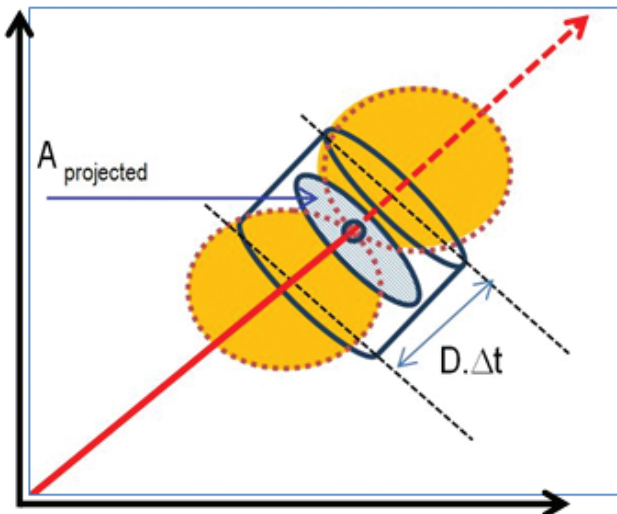
(b) Schematic explanation of determination of burn fraction

Figure 1. Assumptions for burning fraction model used in DSS-DYN.

- The burn fraction for the ith element (F_{i1}) is expressed as:

$$F_{i1} = 2/3 A_i D(t - t_i) / V_i \qquad (1)$$

It has been noted that the Eqn. (1) matches with the expression used in LS-DYNA.[8]

Besides, the burn fraction is computed based on the shock compression, as per the Eqn. (2) with the understanding that detonation initiates once the compressed volumetric strain $(V_O - V)/V_O$ exceeds $P_{CJ}/\rho D^2$, where P_{CJ} is CJ pressure and ρ is the instantaneous density of the element and D is the detonation velocity. Based on this burn fraction is written as:

$$F_{i2} = (V_O - V)/(V_O P_{CJ} / \rho D^2) \qquad (2)$$

The higher of F_{i1} and F_{i2} is F_i in the DSS-DYN.

4. DEFINITION OF BENCHMARK PROBLEM

The benchmark deals with the underwater explosion initiated by a detonation of a spherical shaped PETN having 1 kg mass and radius (r_o) of 50 mm. The functional form of JWL equation of state used for the PETN is as follows:

$$P = A(1 - (\omega / R_1 V)) \exp(-R_1 V) + B(1 - (\omega / R_2 V)) \exp(-R_2 V) + (\omega E / V)$$
$$(3)$$

where V is the relative specific volume v / v_o, which is an independent variable. The specific volumes v and v_o are the inverse of the initial and current densities of the explosive, ρ_o and ρ respectively. A and B are the pressure coefficients. R_1 and R_2 are the principal and secondary parameters to depict the short range and long range behaviour of the explosive respectively. The parameter 'ω' is the fractional part of the energy (E) contributing for the pressure. The parameter values[14] are: ρ_o = 1700 kg/m³, A = 612GPa, B = 21.7GPa, R_1 = 4.92, R_2 = 1.427 and ω = 0.35. The initial internal energy $(E_o) = 8.1 GPa(= 4.7MJ/kg)$.

The geometry is extended to incorporate water medium surrounding PETN to investigate the near-field effects. The inner boundary of water is in contact with the outer boundary of the explosive. The outer boundary radius of water (R_o) is selected as 1000 mm, which ensures the non-reflecting conditions for the water boundary and also captures the essential near-field effects. For the water, Gruneisen equation of state is used.[13]

$$P = \rho_0 C^2 \mu [1 + (1 - \gamma_0 / 2)\mu - a / 2\mu^2]/[1 - (S_1 - 1)\mu] + (\gamma_0 + a\mu)E$$
$$(4)$$

where,

$$\rho_0 = 1000 kg / m^3, C = 1484 m / s, \gamma_0 = 0.11, S_1 = 1.979, a = 3$$

and $E_0 = 0$.

5. RESULTS AND DISCUSSIONS

An integrated axisymmetric finite element analysis including both explosive and water has been carried out. In the axisymmetric analysis, a 90° circular sector is chosen in Z-R plan to represent the hemispherical portion of the geometry.

In this, Z-axis represents the axis of rotation and R axis represents the horizontal symmetric plane. The chosen 90° circular sector is discretised with 559 quadrilaterals for the explosive zone and 858 quadrilaterals for the surrounding water. The following symmetric boundary conditions are applied along the R-axis:

$$U_z = 0 \text{ and } U_R \text{ is unconstrained.} \qquad (5)$$

For the convergency study, the computation mesh size is gradually decreased respecting Courant number $(\Delta x / \Delta l / D) < 0.5$. D is detonation velocity (taken as 8000 m/s). Besides, the mesh size is further refined till solution becomes oscillatory. The minimum mesh size (1.67 mm) has been used through mesh size sensitivity studies and minimum time step (10^{-12} s) is selected for ensuring the applicable stability conditions.[20] The converged results are presented below.

5.1 Detonation Shock Dynamics Responses within Explosive

The spatial and temporal variations of pressure waves are the main quantifiable parameters, which can depict several salient features of DSD. These parameters are presented in 3D graph (Fig. 2). The time to reach DF increases with the radial location. The DF leaves behind burn gases, whose pressure is defined by JWL EOS while crossing the particular location. Thus, pressure field depicts spike followed by plateau pattern. Beyond explosive boundary, shock wave propagation can be seen in this figure. The spatial plots of pressure wave propagation within the explosive, followed by propagation in water are depicted in Fig. 3(a) and Fig. 3(b) respectively, in the form of distributions on a symmetrical plane at a few discrete time intervals. Since the explosive boundary is defined by Lagrangian coordinate, the boundary nodes are attached with the material points, which are indicted by the arrow. It is seen clearly that the explosive boundary expends. Besides these figures confirm that the boundary radius chosen for water envelope all the essential transient responses reflecting the near-field effects as well as the rapid attenuation behaviour in the water generating far-field effects, well within 30ms (Fig. 5 & Fig. 6). These apart, the regularity of mesh during the displacements of fluid particles is ensured through these figures.

In addition, certain special pressure distributions are extracted at a few discrete instants and shown in Fig. 4. The pressure wave propagation has the salient features: (a) pressure waves with the increasing peak values due to the addition of chemical energy in the detonation front and (b) marching towards a saturation state due to the attenuation of pressure wave in a spherical space. The location at which the saturation level is reached depends upon the stored chemical energy of the explosive (E_0). The pressure spikes depict hooping down characteristics in the vicinity of the interface due to the dissipation of pressure energy from the explosive to the adjoining water layers.

The relative motions of the detonation and shock wave fronts are quantified by processing the data. From the computed pressure distributions at various instants (t) (see Fig. 4 for three typical instants), the location of the peak pressure (X), is extracted. Then the speed of a pressure peak, i.e. 'pressure wave velocity', crossing the location (X) is computed as per 'central difference scheme'. The velocity values thus computed at various X values are plotted in Fig. 5. Knowing the position of detonation front at given 't' (D.t), the relative position of pressure peak (ΔX) w.r.t detonation front, is computed as: $\Delta X = (Dt - X)$ at various instants. Thus, the relation' ΔX Vs X', is established and shown in Fig.5 itself. Regarding the velocity distribution, an oscillatory motion of DF and SF with an decreasing trend (after some initial increase) can be seen in the figure. Accordingly, the gap between SF and DF shows an increasing trend. The detonation front velocity is found to be about 7.5 km/s which is close to the analytical value.

(a)

(b)
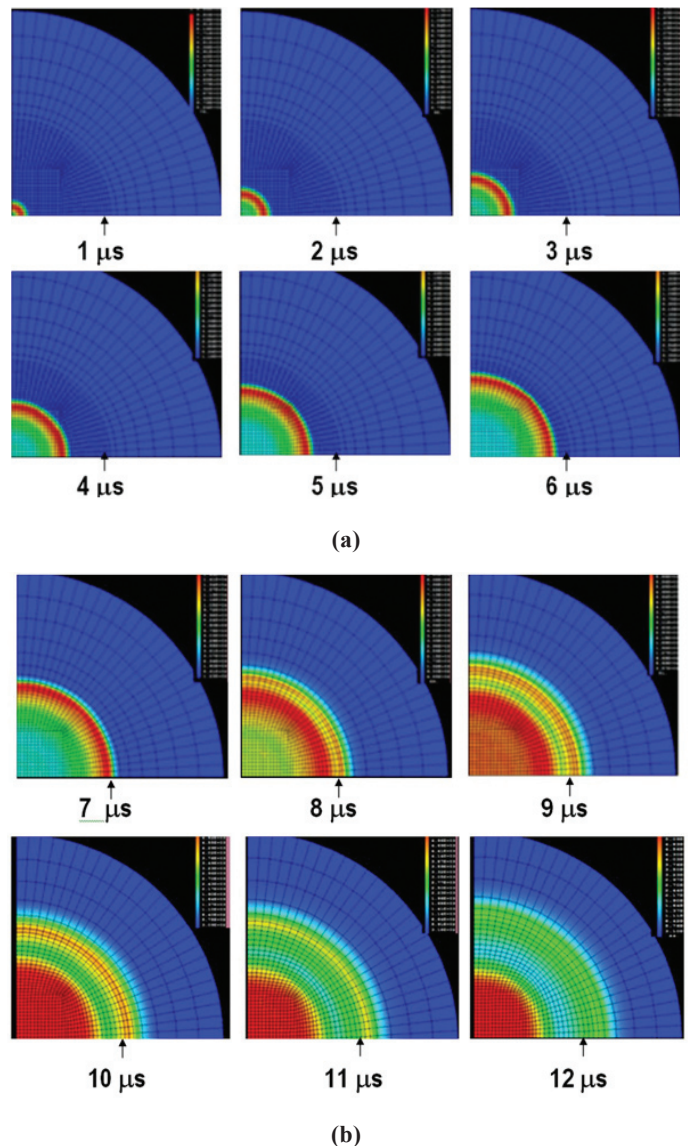
Figure 3. (a) Pressure wave propagation in explosive (arrow shows location of interface), and (b) Pressure wave propagation in water (arrow shows the location of interface).
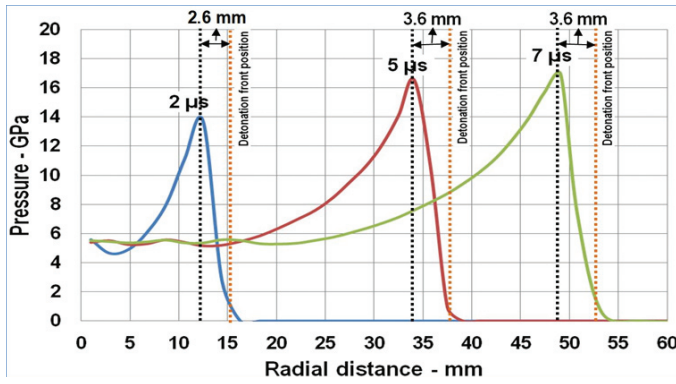
Figure 4. Pressure-time history at discrete radial locations in explosive
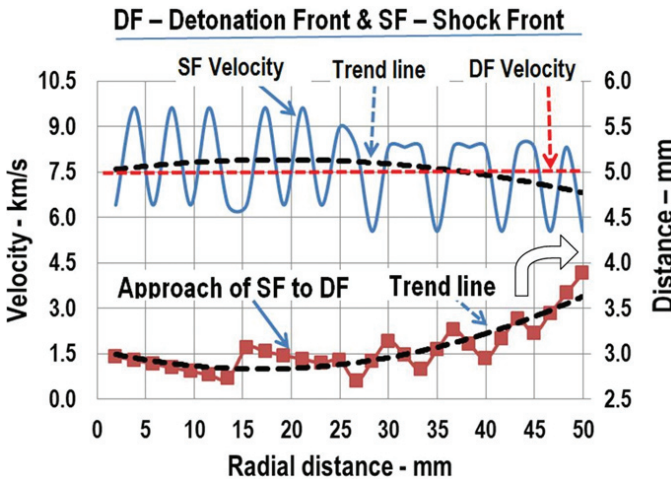
Figure 5. Dynamics of detonation and shock fronts in the explosive.

5.2 Pressure Wave Propagation Characteristics at Interface and Water

From the spatial and temporal pressure distributions computed over the entire domain of computation up to 30ms, the pressure time histories at a few selected radial locations in the boundary layer of explosive (at 49 mm from the centre) and also in the adjoining water layer are extracted and presented in Fig. 6. The rapid drop of pressure peaks with increasing pulse width can be observed. These observations are in-line with the pulse characteristics published in various reference, by Cole[5,23] for example.

Further, it is found that the peak pressure at the interface is lower than the peak pressure at the layer behind the interface at the explosive zone. This is due to the possible attenuation of pressure with the presence of water at much low ambient pressure. This has reflected in the velocity where the peak velocity at the interface line (~2200 m/s) is higher than the velocity (~1700 m/s) at the adjoining layers on the either side of the interface. The peak pressure in the vicinity of the explosive layeradjoining to the water is 17 GPa. This value has shown increasing tend approaching to CJ pressure of 25 GPa with further fine mesh.However,it is practically impossible to model the 'zero thickness interface' in the numerical simulation. Hence, possibly minimum thickness is chosen in the geometrical discretization. Accordingly, there will be pressure attenuation which is reflected in Fig. 6. The averaged pressure in

the adjoining water layer need not be compared with CJ pressure. Once possibly minimum layer thickness is chosen, its effect on the subsequent pressure wave propagation is insignificant, once the impulse is nearly conserved. Measurement of exact pressure at the interface is nearly impossible even in the state-art high speed underwater photography.[6]

Figure 6 indicates that the maximum detonation pressure occurs very close to the explosive boundary, rather than on the interface due to pressure attenuation within the adjoining gaseous and water layers. Hence, the peak pressure value is about 17 GPa. compared to the theoretical value of 25 GPa computed employing the correlation, recommended in 'Mining Technology>Blasting Report': $P_m = 0.2510^{-6} \rho D^2$ for ρ - density of PETN = 1700 kg/m^3 and D-detonation velocity = 7.5 km/s. This prediction is close to the value predicted by LS-DYNA , [Fig. 8(b)].
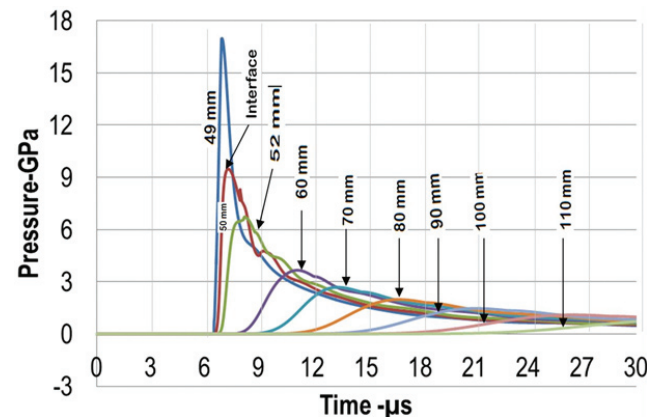
Figure 6. Pressure time histories at the vicinity of interface and water.

5.3 Near-field and Far-field Effects

The near-field effects are produced mainly due to the mechanical interactions of detonation and shock wave fronts at the explosive-liquid interface. The near-field effects on the material depict local behaviour across the structural wall thickness. These can cause damages such as, delamination and disintegration of surface coatings in metals and cratering on the front surface, spallation on the rear surface and perforations in concrete. On the contrary, the far-field effects are produced when the structure offers resistance to shock wave propagation in the liquid. They depict global effects such as rigid body motions of structures with and without deformations and cracking. In the present work, these effects are simulated concurrently by employing robust numerical simulations by controlling the computational mesh size and time step to respect the appropriate stability criteria. Alternatively, analytical solutions are available which are applicable for the regular geometries.Moreover, near and far-field effects are un-coupled while seeking analytical solutions. More details can be found in references.[5, 23 & 14] Figure 6 focusses mainly on near-field effects.

5.4 Energy Distributions

The evolution of mechanical energy in the explosive and water is shown in Fig. 7. Till detonation front arrive at the explosive boundary $(6.6\mu s)$, the internal energy is retained in

the explosive itself. Beyond the explosive starts transmitting its energy to water, causing interface boundary oscillations. which are reflected in the internal energy variations in time scale. Such boundary oscillation behaviour sets in after $9\mu s$ and vanishes (almost) after $21\mu s$. Beyond, the trooping trend of internal energy is observed in association with monotonic increase trend in the energy transmitted to water. Non-reflecting / absorbing boundary conditions are applied for the finite water boundary in the simulation. Besides, compared to the work potential of 4.7 MJ, i.e. the maximum mechanical energy that could be released by 1 kg of PETN in unconfined environment, the energy released by the same 1 kg of PETN in underwater explosion is ~ 1.3 MJ, which is ~30 % of work potential of the PETN Out of 1.3 MJ, only 1 MJ (~20 % of work potential) is transferred to the water that can damage the associated structures / systems.
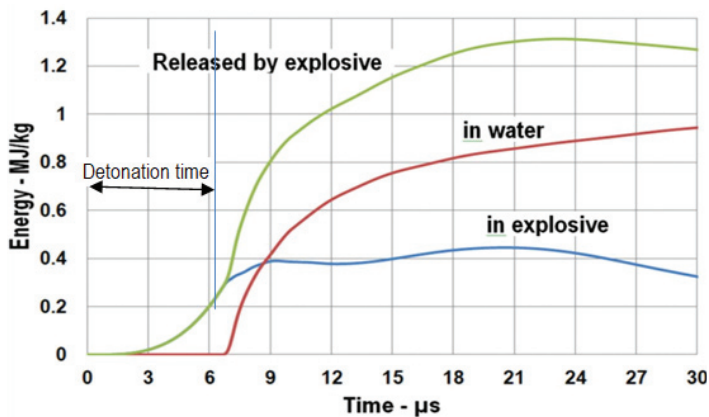
Figure 7. Evolution of energy distributions in PETN and water.

The present numerical simulation deals with infinite water medium which is incompressible. Hence the radial displacement of explosive boundary is insignificant.However, the energy release is strong function of the constrains imposed on the water boundary. This has been observed from TRIG-I series which deal with PETN explosion within water, completely filled in a thin vessel made of stainless-steel.[23] Radial deformation of thin vessels allows the motion of water thereby, higher energy release. In the overall energy balance under static equilibrium condition at the end of the explosion, the strain energy absorbed by the vessel is the measure of maximum mechanical energy release by the explosive. The values determined from 5 tests lie in the range of 2.2-2.6 MJ/kg, compared to 1 MJ/kg in underwater explosion. The details of experimental simulation along with the numerical predictions are presented in.[23]

5.5 Numerical Simulation of DSD with LS-DYNA: Comparison of Results

For the analysis with LS-DYN, the geometrical discretisation of the explosive, equation of state for PETN and water and time step of 10^{-12}s are kept same as per the definition of benchmark problem presented in section-3. The meshing of spherical 50 mm explosive is done by deployment of quadrilateral elements in ALE with variation of element size in two phases viz. for the first 25 mm length of explosive, element size is 1.92 mm and 1.66 mm for the rest. PETN is modelled with MAT_HIGH_EXPLOSIVE_BURN material card with JWL equation of state assigning the beta burn flag equal to 0 to consider the initiation of the detonation either by arrival of detonation front or by volumetric compression, whichever earliest. MAT_NULL material card is used to deploy Gruneisen equation of state for water. The material parameters that are associated with JWL and equations are the same as given
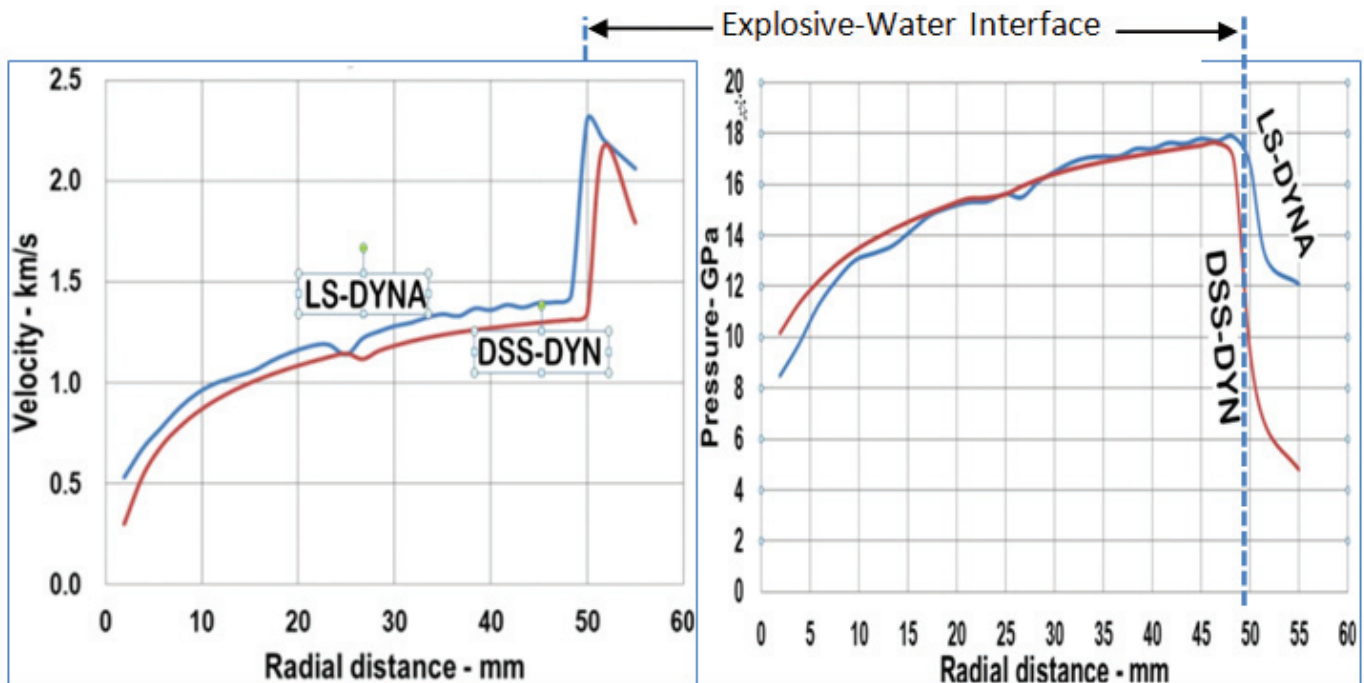
Figure 8. (a) Velocity distribution, and (b) Pressure distribution.

under Eqn. (1) and Eqn. (2) for PETN and water. However, the analysis has been carried out upto 10 μs restricting the simulation of DSD propagation within the explosive zone. The LS-DYNA and DSS-DYN predictions of peak velocity values at the nodal points are compared in Fig. 8(a) and peak pressure values at the element centroids along the symmetric line are compared in Fig. 8(b). The marginal differences observed in the predictions are mainly due to the homogenization of pressure fields in the burn and un-burnt zones. Relatively a large difference has been observed in the water region in the vicinity of interface. This is mainly due to the deviation in arrival times of shock wave fronts at the interface, apart from possible discretization error in the hydrodynamic computations by finite element simulations. Further, it is experienced that the computational time consumed by DSS-DYN is typically less than an hour and LS-DYNA took about 3 hours for a run.

6. CONCLUSIONS

The DSD scenario has been simulated precisely both in time and space scales. JWL equation of state for explosive along with the simple algorithm developed for determining the burnt fraction in the explosive zone is well suited for the integrated/ coupled finite element analysis.The prediction of important DSD parameters by DSS-DYN shows satisfactory comparison with the LS-DYNA with lesser computational time. The energy distribution indicates that only about 30 % of stored chemical energy has ability to deliver mechanical work on the fluid, of which 70 % is transmitted to the surrounding water.It is further observed that the energy release scenario is strong function of the conditions imposed on the water boundary. This has been experimentally confirmed.These data provide important input for the design of energy absorbing mechanisms as well as damage assessment of the structures involved in an underwater explosion.

Assessment of DSS-DYN with reference to LS-DYNA employing more examples under varied experimental conditions and extension of DSS-DYN for the analysis of 3D geometries including the shock-structure interactions is the future work of authors.

REFERENCES

1. Zhi-Yue, Liu. Overdriven detonation phenomenon and its application to ultrahigh pressure generation, Kumamoto University, 2001. (PhD Thesis).
doi:10.1117/12.42434
2. Craig, M. Tarver. Condensed matter detonation : Theory and practice,in :Shock Waves Sci. Technol. Libr, Springer Publication,2012,339–372.
doi:10.1007/978-3-642-22967-1_6
3. Bdzil, J.B. & Stewart, D.S. Modeling two-dimensional detonations with detonation shock dynamics, Phys. Fluids A Fluid Dyn, 1989, **1**, 1261-1267.
https://aip.scitation.org>doi>abs>1.857349
4. Aslam, T.D. & Stewart, D.S. Detonation shock dynamics and comparisons with direct numerical simulation, combust. Theory Model, 1999, **3**, 77–101.
doi:10.1088/1364-7830/3/1/005
5. Cole, R.H. Underwater explosions, Princeton University Press, Princeton, NJ, 1948.
6. Gabi, Ben-Dor; OzerIgra & Tov, Elperin. Handbook on shock wave, Elsevier, 2001.
7. ANSYS. AUTODYN User Manual Version 15.0 ANSYS Inc., Canonsburg, PA,2015.
8. Livermore Software Technology Corporation (LSTC). LS-DYNA Keyword User's Manual Ver. R9.0. Livermore Software Technology Corporation, Livermore, 2016.
9. ABAQUS User Manual Version 6.14 Hibbitt, Karlsson & Sorensen, Inc.,2015.
10. MSC/DYTRAN User's Manual V4, The MacNeal-Schwendler Corporation,2009.
11. Wang, C.; Ye, T & Ning, J. Numerical simulation of the detonation of condensed explosives. *Mod. Phys. Lett.*, 2009, B**23**, 285-288.
doi:10.1142/S0217984909018217
12. Wu, C.; Fattori, G; Whittaker, A. & Oehlers, D. Investigation of air-blast effects from sphericaland cylindricalshaped charges. *Int. J. Protective Struct.*, 2010, **1**, 345–362.doi:10.1260/2041-4196.1.3.345
13. Molyneaux, T.C.K.; Li, L.Y. & Firth, N. Numerical simulation of underwater explosions. *Comput. Fluids*, 1994, **23**, 903–911.0045-79.30(94)E0009-9
14. Nastasescu, V. & Bârsan, G. Upon analytical and numerical calculus of the main parameters of the detonatin process. *Bul. AGIR*, 2015, 13–21.
https://www.agir.ro >buletine
15. Cheng, C.W. & Hung, S.Ji. Numerical simulation of near-field explosion. *J. Appl. Sci. Eng*, 2013, **16**, 61–67.
doi:10.6180/jase.2013.16.1.09
16. Shin, J.; Whittaker, A.S.; Cormie, D & Wilkinson, W. Numerical modeling of close-in detonations of high explosives. *Eng. Struct.,* 2014, **81**, 88–97.
doi:10.1016/j.engstruct.2014.09.022
17. Kira, A.; Fujita, M. & Itoh, S. Underwater explosion of spherical explosives. *J. Mater. Process. Technol.*, 1999, **85**, 64–68.
doi:10.1016/S0924-0136(98)00257-X
18. Tong-hui, Yang & Cheng, Wang. Numerical simulation study on sympathetic detonation in stages. *Def. Technol.*
doi:10.1016/j.dt.2021.08.009
19. Menikoff , Ralph. JWL equation of state, Report No. LA-UR-15-29536, LANL,USA, 2015.
doi:10.2172/1229709
20. Urtiew, P.A. & Hayes, B. Parametric study of the dynamic JWl-Eos, Combust. *Shock Waves*, 1991, **27**, 505–514.
doi:10.1007/BF00789568
21. Koli,Sourabh;Chellapandi,P.;Rao,Bhaskara,Lokavarapu & Sawant, Akshay. Study on JWL equation of state for the

numerical simulation of near-field and far-field effects in underwater explosion scenario, Engineering Science and Technology. *An Int. J.*, 2020, **23**(4), 758-768.
doi:10.1016/j.jestch.2020.01.007

22. Ahmed, Hawass; Ahmed, Elbeih & Hosam, E. Mostafa. Theoretical and experimental study of underwater explosion performance of selected explosive compositions, 2019, IOP Conf. Ser.: Mater. Sci. Eng. 610 012061.
doi:10.1088/1757-899X/610/1/012061

23. Chellapandi, P; Chetal, S.C. & Baldev, Raj. Structural integrity assessment of reactor assembly components of a pool type sodium fast reactor under core disruptive accident - Part 1: Development of computer code and validations. *J. Nuclear Technol.*, 2010, **172**, 01-15.
doi:10.13182/NT10-A10878

24. Bdzil, J.B.; Stewart, D.S. & Jackson, T.L. Program burn algorithms based on detonation shock dynamics: Discrete approximations of detonation flows with discontinuous front models. *J. Comput. Phy.*, 2001, **174**, 870–902.
doi:10.1006/JCPH.2001.6942 Corpus ID: 17112897

CONTRIBUTORS

Dr P. Chellapandi is a Distinguished Alumni of IIT Madras with MTech and PhD in Applied Mechanics. He got his DS from AMET University, Chennai. He is a Fellow of Indian National Academy of Engineering. Currently, he is an INAE Distinguished Professor at IIT-Madras Chennai. His major specializations are Fast Reactor Design & Technology in general and High Temperature Design and Fast Transient Fluid Structure Interaction Dynamic in particular.
For this work, he has performed numerical simulation and benchmark validation, apart from overall contribution.

Dr Lakshmana Rao is a Professor in the Department of Applied Mechanics at IIT Madras. He has obtained his bachelors and master's degree from the department of civil engineering at IIT Madras and DS in mechanics of materials from Massachusetts Institute of Technology. His areas of specialization include solid mechanics in general and damage mechanics, impact mechanics, fracture Mechanics and finite element analysis, in particular.
For this work, he contributed for the analytical formulations and helped in preparation of the manuscript.